Segmented golden ratio radial reordering with variable temporal resolution for dynamic cardiac MRI

Fei Han, Ziwu Zhou, Stanislas Rapacchi, Kim-Lien Nguyen, J. Paul Finn, Peng Hu

Published in final edited form as:

Magn Reson Med. 2016 July ; 76(1): 94–103. doi:10.1002/mrm.25861.

Segmented Golden Ratio Radial Reordering with Variable Temporal Resolution for Dynamic Cardiac MRI

Fei Han, M.S.[1,2], **Ziwu Zhou, B.S.**[1,2], **Stanislas Rapacchi, Ph.D.**[1], **Kim-Lien Nguyen, M.D.**[1,4], **J. Paul Finn, M.D.**[1], and **Peng Hu, Ph.D.**[1,3,*]

[1]Department of Radiological Sciences, David Geffen School of Medicine, University of California, Los Angeles, CA

[2]Department of Bioengineering, University of California, Los Angeles, CA

[3]Biomedical Physics Inter-Departmental Graduate Program, University of California, Los Angeles, CA

[4]Division of Cardiology, VA Greater Los Angeles Healthcare System and David Geffen School of Medicine, University of California, Los Angeles, CA

Abstract

Purpose—Golden ratio (GR) radial reordering allows for retrospective choice of temporal resolution by providing a near-uniform k-space sampling within any reconstruction window. However, when applying GR to ECG-gated cardiac imaging, the k-space coverage may not be as uniform because a single reconstruction window is broken into several temporally isolated ones. We seek to investigate the image artifacts caused by applying GR to ECG-gated cardiac imaging and propose a segmented GR method to address this issue.

Methods—Computer simulation and phantom experiments were used to evaluate the image artifacts resulting from three k-space sampling patterns, i.e. uniform radial, conventional GR and the segmented GR. 2D and 3D cardiac CINE images were acquired in 7 healthy subjects. Imaging artifacts due to k-space sampling non-uniformity were graded on a 5-point scale by an experienced cardiac imaging reader.

Results—Segmented GR provides more uniform k-space sampling that is independent of heart-rate variation than conventional GR. Cardiac CINE images using segmented GR have significantly higher and more reliable image quality than conventional GR.

Conclusion—Segmented GR successfully addresses the non-uniform sampling that occurs with combining conventional GR with ECG gating. This technique can potentially be applied to any ECG-gated cardiac imaging application to allow for retrospective selection of a reconstruction window.

[*]Correspondence to: Peng Hu, PhD, Department of Radiological Sciences, 300 UCLA Medical Plaza Suite B119, Los Angeles, CA 90095, penghu@mednet.ucla.edu.

Introduction

In dynamic MRI acquisitions, golden ratio (GR) radial sampling (1,2) is widely known because it allows for retrospective selection of temporal window and temporal resolution. In these methods, the angles of the k-space radial spokes are advanced in each repetition time (TR) by the golden ratio conjugate of 180° (i.e. 0.618*180 =111.25°) such that the angular distribution of the radial spokes within any given temporal window is approximately uniform. This uniformity enables arbitrary and retrospectively defined temporal resolution during image reconstruction. GR radial sampling has been applied in many abdominal, cardiothoracic and neurological imaging applications (3–7). However, its application in cardiac MRI has been mostly focused on real time cardiac CINE imaging, where the data acquisition is not synchronized with the electrocardiogram (ECG)(8,9). For most cardiac MRI applications where the k-space data acquisition is segmented and gated to ECG, the angular distribution of the radial spokes for a given temporal window is not necessarily uniform because a single reconstruction window is broken into several temporally isolated ones. As a result, for any given temporal window, the radial k-space coverage may not be as uniform as conventional non-segmented GR radial acquisitions, a problem that has been recently recognized (10–12). Hence, we seek to investigate the k-space sampling pattern and image artifacts caused by applying GR radial acquisition to segmented ECG-gated cardiac MRI applications and propose a modified GR radial technique to address this issue.

Theory

The angle α of each radial spoke in the conventional GR method is calculated as:

$$\alpha_{n+1}=mod\left[\left(\alpha_n+180^\circ * \frac{\sqrt{5}-1}{2}\right), 180^\circ\right] \quad \text{(Eq.1)}$$

Winklemann et al. have demonstrated in (1) that such radial profile order ensures an approximately uniform sampling of k-space with arbitrary temporal window length and window position. However, if the data is chosen from multiple isolated subsets of all the measured spokes, as in the case of dynamic cardiac imaging with ECG-gating and k-space segmentation, it is likely that the spokes from these isolated subsets are clustered in certain sectors instead of being uniformly distributed over the entire k-space (Figure 1a). We therefore, hypothesize that the degree of k-space non-uniformity is dependent on the number of k-space radial spokes between two image reconstruction windows (i.e. heartbeat duration in ECG-gated cardiac applications). If the first radial spoke of a new heartbeat falls within the proximity of a previously acquired one, then the remaining radial spokes in this heartbeat will be clustered with the previously acquired ones because all of them are advanced by the same angle of 111.25°. Such clustering of radial spokes may lead to imaging artifacts due to non-uniform k-space sampling and under-sampling in certain k-space regions.

The k-space sampling non-uniformity may be controlled by choosing a proper number of k-space radial spokes between two reconstruction windows to mitigate the clustering of radial spokes. However, in ECG-gated cardiac applications, this number is determined by the

heartbeat duration of the subject, which is not only variable during the scan and but also beyond the control of the scan operator. To address this problem, we propose a segmented GR radial acquisition scheme to completely avoid the k-space sampling non-uniformity issue when applying GR in dynamic cardiac MRI applications, such as cardiac CINE. In the proposed segmented GR radial method (Eq. 2), the entire k-space is first divided into N segments and the angle of the radial spokes is advanced according to the golden ratio conjugate of the current k-space segment that is being acquired, rather than the golden ratio conjugate of 180°, which is the case in conventional GR radial sampling. Hence, the angle increment is not a fixed angle, but rather depends on the total number of segments N, which is the number of heartbeats in a cardiac CINE acquisition, and the index of the k-space segment s=0,1,2…N.

$$\alpha_{n+1}(s)=mod\left[\left(\alpha_n+\left({}^{180^\circ}\!/_{N}\right)*\frac{\sqrt{5}-1}{2}\right),{}^{180^\circ}\!/_{N}\right]+s*\left({}^{180^\circ}\!/_{N}\right) \quad \text{(Eq.2)}$$

In the example shown in Figure 1b, the entire k-space is divided into 4 segments. The angle of the radial spokes in each heartbeat is advanced according to Eq. 2 within the current segment only until the next ECG trigger signal. Since each segment is sampled with radial spokes in a golden ratio manner, any subset of these measurement forms a near-uniform sampling of the current segment and together with other segment, forms a near-uniform sampling of the entire k-space.

Methods

Computer Simulation

The proposed segmented GR method was compared with uniform radial sampling and conventional GR sampling using computer simulation. Four different radial data acquisition strategies were simulated. In non-ECG-gated simulations, the angles of K radial spokes (K=60, 96, 144 and 192) were simulated using a) uniform sampling (strategy 1) where α_n = 180° * *n/K*; and b) conventional GR sampling (strategy 2) described in Eq. 1. For the case with ECG-gating and k-space segmentation, the radial spoke angles were calculated for 12 simulated heart-beats, using c) conventional GR radial (strategy 3) shown in Eq. 1; d) the proposed segmented GR radial (strategy 4) shown in Eq. 2. Subsequently, a subset of k=5, 8, 12 and 16 spokes were chosen retrospectively from each of the 12 heartbeats so that the total number of radial spokes in the simulated ECG-gated cases were identical to the non-ECG-gated cases. In order to test our hypothesis that the degree of k-space non-uniformity is dependent on the number of k-space spokes between two image reconstruction windows in strategy 3, the number of radial spokes in each simulated heartbeat was varied from M=161~240. This is to simulate the cases of 2D cardiac CINE applications where TR=4ms and the average heart rate variation is from 60 to 100bpm.

The angles of the selected radial spokes for each of the four simulated 2D radial k-space data sets were sorted (from smallest to largest) as β_i^{sorted}, i=1 … K. The average angular difference between the current and two neighboring radial spokes were calculated as

$d_i = (\beta_{i+1}^{sorted} - \beta_{i-1}^{sorted}) / 2$ and plotted against the sorted radial spoke index i to evaluate the local angular sampling density. The standard deviation of the local angular sampling density d_i was used to quantitatively assess the global angular uniformity of k-space sampling. A zero standard deviation suggests a perfectly uniform radial k-space, which is the case for non-GR radial sampling. A numerical Shepp-Logan phantom was used in the simulation to investigate the image artifacts resulting from these sampling patterns.

Phantom Study

A 2D-radial based balanced steady-state free precession (bSSFP) sequence was modified to implement the four different acquisition schemes that were tested in our computer simulation. In the conventional GR radial acquisition, there is a large angular increment of 111.25° in each successive TR, which may cause strong eddy current related artifacts in bSSFP acquisitions (13). To demonstrate this, a reordered GR sampling (strategy 5) was also implemented in our sequence where the angles of the radial spokes were identical to the conventional GR but sampled in a sequential order from 0 to 180° with much smaller increment in angle of the radial spokes from TR to TR.

All phantom imaging was performed using a 1.5T MRI scanner (Avanto, Siemens Medical Solutions) with 16 channel head coil, on a standard American College of Radiology (ACR) MRI stationary phantom. Sequence parameters include: TE/TR=2.0/4.0ms; Base Resolution=256. Five 2D bSSFP radial data sets (192 radial spokes) were acquired based on the aforementioned acquisition strategies 1–5. In the ECG-gated acquisitions (strategy 3 and 4), a simulated ECG signal was generated with 800ms cardiac cycle length and the data was acquired in 12 heartbeats. A temporal window that contains 16 radial spokes was placed retrospectively on all the cardiac cycles so that a total number of 192 radial spokes were selected for image reconstruction. All images were reconstructed offline using a Matlab program that performs k-space gridding and inverse Fourier transform. K-space sampling density was compensated during image reconstruction in all computer simulation, phantom and in-vivo imaging experiments. For the case of uniform sampling (strategy 1) where the angular density is constant, the compensation weights was calculated as the distance between the sampling point and the k-space center point. For all other cases (strategy 2–5), the weight of each k-space sampling point was calculated as its distance to k-space center point multiplies by the local angular sampling density of the radial spoke it belongs to. The local angular sampling density has been previously defined in the computer simulation section as the average angular difference between the current and the two neighboring radial spokes.

In-Vivo study

Breath-held, ECG-gated 2D radial cardiac CINE images were acquired on seven healthy volunteers using the conventional GR and the segmented GR reordering scheme. Images were acquired in five different orientations for each subject, including three in the cardiac short axis (base, mid and apex of the left ventricle), one in the vertical long axis and one in the horizontal long axis. Sequences used in in-vivo studies were identical to those used in the ECG-gated static phantom studies (strategy 3 and 4). The total acquisition time of each

sequence was 10±2 seconds (12 heartbeats, average heart rate: 60–90bpm). In addition, breath-held, ECG-gated 3D cardiac CINE images using a stack-of-stars radial trajectory were also acquired to assess any image artifacts caused by the k-space non-uniformity in 3D acquisitions. The 3D stack-of-stars acquisition covered the whole ventricle in cardiac short axis, with the following sequence parameters: TE/TR=1.7/3.4ms; partitions=16, line resolution=256, 6/8 partial Fourier in Kz direction, total acquisition time=20–24sec, temporal resolution = 140–160ms.

The acquired 2D and 3D radial cardiac CINE images were subjectively scored by an experienced reader (> 4 years of experience in cardiac MRI), who was blinded to the acquisition strategy, to evaluate the degree of image artifacts due to k-space sampling non-uniformity. The scores were given on a scale of 1–5 (1: severe streaking artifact rendering the image non-diagnostic; 2: moderate streaking such that myocardial borders are poorly defined and regional wall motion cannot be assessed, rendering the image non-diagnostic; 3: mild streaking such that myocardial borders are well-defined, but the definition of fine structures is compromised; 4: minimal streaking but does not affect identification of fine structure, regional wall motion, and overall cardiac function; 5: no observable streaking artifact, diagnostic quality without imaging degradation). The subjective image quality scores were compared using a Wilcoxon signed-rank test. $P < 0.05$ is considered statistically significant.

Results

Computer Simulation

The k-space sampling patterns and the local angular sampling densities based on the radial sampling strategies 1 to 4, for the case of K=60 (k=5, 12 simulated heartbeats, 200 radial spokes per heartbeat (M=200) for strategies 3 and 4) are shown in Figure 2. The k-space global angular sampling uniformity, as assessed by the standard deviation of the local angular sampling densities, are listed in Table 1 for cases of K=60, 96, 144 and 192. Standard uniform sampling (strategy 1) provided the most uniform coverage of k-space with identical local angular sampling density for all 60 radial spokes. However, there was no flexibility for varying the reconstructed temporal resolution. The conventional non-ECG-gated GR radial method (strategy 2) provided an approximately uniform sampling of k-space with a small variation in local angular sampling density of 2°–5°. However, conventional GR sampling in an ECG-gated acquisition (strategy 3) resulted in large variation of local angular sampling density between 0.4°–23° and poor sampling uniformity (standard deviation of 6.73 in Table 1). The proposed segmented GR radial method with ECG-gating (strategy 4) offered highly uniform k-space sampling that is comparable to the conventional GR without ECG-gating.

The k-space global angular uniformities for ECG-gated conventional GR (strategy 3) and the segmented GR (strategy 4) using M=161–240 (K=96), calculated as the standard deviation of the local angular sampling density d_i, are shown in Figure 3. The k-space global sampling uniformity for ECG-gated conventional GR varied significantly (0.58° to 4.41°) depending on the number of radial spokes acquired in each heartbeat and the length of each individual cardiac cycle. However, the segmented GR provided a much improved k-space global

uniformity of 0.46° and is independent of the number of radial spokes in each heartbeat. Figure 3b–e shows the reconstructed images using the k-space sampling pattern of the proposed segmented GR and conventional ECG-gated GR when M=178, 189 and 225. Severe streaking artifacts were present in the ECG-gated conventional GR images due to non-uniform k-space sampling while the segmented GR generated images with minimum streaking artifacts in all simulated scenarios.

Phantom Study

Figure 4 shows the five reconstructed images in the static phantom scans. Similar to our computer simulation results, the conventional GR was associated with severe streaking image artifacts when the acquisition was gated to ECG (Figure 4d) and the artifacts were essentially eliminated using the segmented GR approach (Figure 4e). Figures 4b–c demonstrate the potential benefit of having smaller angle increments in each successive TR. With the conventional GR technique, due to the large 111.25° angle increment, there were considerable image artifacts (red arrows) and these artifacts were eliminated using the re-ordered GR acquisition (strategy 5) because the eddy current related phase accruals were much smaller due to the much smaller angle increment for each successive TR.

In-Vivo Study

Figure 5 shows selected phases of 2D ECG-gated cardiac short axis CINE images on a healthy volunteer using the conventional GR and the proposed segmented GR methods. Both CINE images were reconstructed into 18 cardiac phases with temporal resolution of 40ms. Due to non-uniform sampling of k-space, severe streaking artifacts were present in the conventional GR images, which compromised the delineation of the overall anatomy. The proposed segmented GR method offered much improved image quality in terms of artifacts even though the same number of radial views was used for reconstruction.

Figure 6 shows examples of breath-held 2D cardiac CINE images in the short axis, vertical long axis and horizontal long axis, from a healthy volunteer. With conventional GR sampling, the subtle heart rate variation during each scan led to small alterations in the number of radial spokes within each heartbeat (182±9 spokes per heartbeat), which in turn resulted in significant variations in the image quality. However, the proposed segmented GR method was able to provide images with minimum streaking artifacts despite similar heart rate variation across the segmented GR radial scans. These results agree well with our computer simulation results in Figure 3. Figure 7 shows selected phases/slices of the breath-held 3D cardiac CINE images on four healthy subjects. Similar to the 2D cardiac CINE images, the image quality of the conventional ECG-gated GR was not reliable as it heavily depends on the subject’s heart rate as well as pulse sequence parameters. The images on subjects 1 & 3 were completely non-diagnostic due to severe streaking artifacts. The proposed GR method provided images with diagnostic quality and minimum streaking artifacts in all four subjects. The relative uniform k-space sampling pattern in the proposed GR method is less dependent on variations in heart rate and pulse sequence parameters.

Subject image quality scores on the 2D and 3D cardiac CINE images are listed in Table 2. The score of the proposed segmented GR method is significantly higher than conventional

GR (4.2±0.5 vs. 1.7±0.8, p=0.01). In addition, the standard deviation of the image quality scores of the proposed segmented GR method is smaller than the conventional GR, suggesting that image quality is more reliable.

In Figure 8, one of the 2D cardiac CINE dataset using the proposed segmented GR method is reconstructed into two different sets of images: a) 24 cardiac phases with a temporal resolution of 33ms; and b) 8 cardiac phases with temporal resolution of 100ms. Both sets of images have minimal streaking artifacts. Based on visual impressions, the 33ms image set had less image blurring than the 100ms image set at ventricular systole due to its shorter temporal footprint, although it was also noisier than the 100ms image set, which was expected due to the fewer radial spokes used. This example demonstrates the flexibility of retrospectively defined temporal resolution afforded by the proposed segmented GR method.

Discussion

In this paper, we propose a segmented GR radial method for ECG-gated k-space segmented acquisitions and demonstrate its advantage of more uniform and efficient radial k-space sampling over conventional GR radial sampling while maintaining the desirable ability to retrospectively define the temporal window during image reconstruction. The proposed method may be applied to dynamic cardiac imaging applications, such as cardiac CINE imaging and phase-contrast MRI. An additional benefit of the segmented GR radial technique is the potential reduction of eddy current-related image artifacts during bSSFP acquisition, which is related to the reduction of the angular increment from TR to TR. Because bSSFP is commonly used in cardiac MRI, this side benefit would be of value. Further, the ability to retrospectively select the temporal window during image reconstruction would be beneficial in cases of dysrhythmias and/or motion related artifacts whereby certain structures are better defined in one phase of the cardiac cycle, but less well-defined in another.

The computer simulation result shown in Figure 3 confirms our hypothesis that when applying conventional GR to ECG-gated, k-space segmented acquisitions, the k-space sampling uniformity is dependent on the number of radial spokes between each image acquisition window (i.e. heartbeat duration). Although it is technically possible to choose the proper number of radial spokes within a single heart beat based on the simulation result in Figure 3a, in order to avoid severe k-space sampling non-uniformity (e.g. M=178), it is not a practical option for a variety of reasons. The heart rate of the subject is beyond the control of the scan operator and even a small change in heart rate could result in dramatic changes in the k-space sampling uniformity. However, the proposed segmented GR method has reliable performance in terms of k-space sampling uniformity that is independent of the heart rate.

In anatomical cardiac imaging applications, the acquisition window is usually defined prospectively to limit the data acquisition to the quiescent cardiac phase where myocardial motion is minimal. Defining the quiescent phase for each subject is usually done prior to image acquisition and thus cannot be adapted to the beat-to-beat variation in heart rate during the single image acquisition. Improperly defining the quiescent phase may potentially lead to motion artifact in the images and, if severe, may require a repeated scan. The

proposed segmented GR method provides a potential solution by enabling the acquisition window to be retrospectively defined. The acquisition window can be determined using either off-line analysis of the recorded ECG signal (14) or by using self-gating techniques where k-space data are used to estimate the cardiac motion (15–17).

In this work, we applied the proposed segmented GR method to cardiac CINE applications using 2D radial and 3D stack-of-stars trajectories. The principle of the proposed method could also be applied to 3D radial “koosh ball” trajectory by first segmenting the radial sphere into multiple 2D regions and perform 2D golden ratio (2) reordering inside each 2D region within a heartbeat.

The images generated using computer simulations, phantoms, and in-vivo studies were all reconstructed using standard k-space gridding and Fourier transform. Several recent non-linear image reconstruction methods (18–20) take advantage of multiple coil arrays and image sparsity to remove aliasing and streaking artifacts in under-sampled k-space acquisitions. Although these algorithms, in theory, are capable of estimating the missing k-space data and reconstruct any under-sampled k-space data, their performance is highly dependent on the specific k-space sampling pattern. Chan et al. compared the performance of compressed sensing reconstruction under different radial sampling schemes and concluded that while Cartesian under-sampling trajectories require randomness to generate incoherent artifacts for compressed sensing, radial projections with random angles in radial under-sampling is not desirable compared with those having evenly spaced projections (6). Therefore, we expect our proposed segmented GR method to outperform conventional ECG-gated GR even when these advanced non-linear image reconstruction methods are used. The strengths of the proposed segmented GR method lie in its ability to provide a more stable and uniform k-space sampling pattern. However, additional simulations and testing under different clinical conditions is warranted to further validate our expectations.

The computer simulation, phantom and in-vivo studies in this study were all based on prospectively ECG-triggered cardiac CINE acquisitions, which may not cover the entire cardiac cycle due to the need for “dummy pulses” at the end of the heart beat to accommodate heart rate variations. It is well known that retrospectively ECG-gated acquisitions can overcome this problem. However, in this study, we used the prospectively ECG-triggered acquisition because the number of radial spokes acquired in each heartbeat is constant, which allows us to better study the behavior of the k-space sampling non-uniformity and its relationship with the heart rate variations. For retrospective ECG-gated acquisitions, the same k-space sampling non-uniformity issue also exists and our segmented GR radial technique would be equally applicable to address this issue.

In summary, we investigated the k-space sampling pattern and the resulting image artifacts when applying conventional GR to ECG-gated cardiac imaging. We found that the degree of k-space non-uniformity is dependent on the number of k-space spokes between two image reconstruction windows (i.e. heartbeat duration in ECG-gated cardiac applications). Our proposed segmented GR method successfully addresses the non-uniform sampling issue when combining conventional GR with ECG gating and can be potentially applied to any ECG-gated cardiac imaging applications, including CINE and flow imaging as well as

cardiac phase-resolved coronary MRI, to allow for retrospective selection of temporal resolution.

Supplementary Material

Refer to Web version on PubMed Central for supplementary material.

Acknowledgments

P.H. acknowledges research support from National Institutes of Health (1R21HL113427).

References

1. Winkelmann S, Schaeffter T, Koehler T, Eggers H, Doessel O. An optimal radial profile order based on the Golden Ratio for time-resolved MRI. IEEE transactions on medical imaging. 2007; 26(1): 68–76. [PubMed: 17243585]
2. Chan RW, Ramsay EA, Cunningham CH, Plewes DB. Temporal stability of adaptive 3D radial MRI using multidimensional golden means. Magnetic resonance in medicine. 2009; 61(2):354–63. [PubMed: 19165897]
3. Feng L, Grimm R, Tobias Block K, Chandarana H, Kim S, Xu J, Axel L, Sodickson DK, Otazo R. Golden-angle radial sparse parallel MRI: Combination of compressed sensing, parallel imaging, and golden-angle radial sampling for fast and flexible dynamic volumetric MRI. Magnetic Resonance in Medicine. 2013 Sep; 72(3):707–717. [PubMed: 24142845]
4. Lin W, Guo J, Rosen MA, Song HK. Respiratory motion-compensated radial dynamic contrast-enhanced (DCE)-MRI of chest and abdominal lesions. Magnetic resonance in medicine: official journal of the Society of Magnetic Resonance in Medicine / Society of Magnetic Resonance in Medicine. 2008; 60(5):1135–46.
5. Liu J, Glenn OA, Xu D. Fast, free-breathing, in vivo fetal imaging using time-resolved 3D MRI technique: preliminary results. Quantitative imaging in medicine and surgery. 2014; 4(2):123–8. [PubMed: 24834424]
6. Chan RW, Ramsay EA, Cheung EY, Plewes DB. The influence of radial undersampling schemes on compressed sensing reconstruction in breast MRI. Magnetic resonance in medicine: official journal of the Society of Magnetic Resonance in Medicine / Society of Magnetic Resonance in Medicine. 2012; 67(2):363–77.
7. Kecskemeti S, Johnson K, Wu Y, Mistretta C, Turski P, Wieben O. High resolution three-dimensional cine phase contrast MRI of small intracranial aneurysms using a stack of stars k-space trajectory. Journal of magnetic resonance imaging: JMRI. 2012; 35(3):518–27. [PubMed: 22095652]
8. Hansen MS, Sørensen TS, Arai AE, Kellman P. Retrospective reconstruction of high temporal resolution cine images from real-time MRI using iterative motion correction. Magnetic resonance in medicine: official journal of the Society of Magnetic Resonance in Medicine / Society of Magnetic Resonance in Medicine. 2012; 68(3):741–50.
9. Zhang S, Joseph AA, Voit D, Schaetz S, Merboldt K-D, Unterberg-Buchwald C, Hennemuth A, Lotz J, Frahm J. Real-time magnetic resonance imaging of cardiac function and flow-recent progress. Quantitative imaging in medicine and surgery. 2014; 4(5):313–29. [PubMed: 25392819]
10. Krämer M, Herrmann KH, Biermann J, Reichenbach JR. Retrospective reconstruction of cardiac cine images from golden-ratio radial MRI using one-dimensional navigators. Journal of Magnetic Resonance Imaging. 2014; 40(2):413–422. [PubMed: 24895008]
11. Edelman RR, Giri S, Murphy IG, Flanagan O, Speier P, Koktzoglou I. Ungated radial quiescent-inflow single-shot (UnQISS) magnetic resonance angiography using optimized azimuthal equidistant projections. Magnetic resonance in medicine. 2014; 72(6):1522–9. [PubMed: 25257379]

12. Kawaji K, Foppa M, Roujol S, Akçakaya M, Nezafat R. Whole heart coronary imaging with flexible acquisition window and trigger delay. PloS one. 2015; 10(2):e0112020. [PubMed: 25719750]
13. Wundrak S, Paul J, Ulrici J, Hell E, Rasche V. A Small Surrogate for the Golden Angle in Time-Resolved Radial MRI Based on Generalized Fibonacci Sequences. IEEE transactions on medical imaging. 2014 Dec 18.
14. Wang Y, Watts R, Mitchell I, Nguyen TD, Bezanson JW, Bergman GW, Prince MR. Coronary MR angiography: selection of acquisition window of minimal cardiac motion with electrocardiography-triggered navigator cardiac motion prescanning–initial results. Radiology. 2001; 218(2):580–5. [PubMed: 11161182]
15. Larson AC, White RD, Laub G, McVeigh ER, Li D, Simonetti OP. Self-gated cardiac cine MRI. Magnetic resonance in medicine. 2004; 51(1):93–102. [PubMed: 14705049]
16. Pang J, Sharif B, Fan Z, Bi X, Arsanjani R, Berman DS, Li D. ECG and navigator-free four-dimensional whole-heart coronary MRA for simultaneous visualization of cardiac anatomy and function. Magnetic resonance in medicine: official journal of the Society of Magnetic Resonance in Medicine / Society of Magnetic Resonance in Medicine. 2014; 72(5):1208–17.
17. Kolbitsch C, Prieto C, Schaeffter T. Cardiac functional assessment without electrocardiogram using physiological self-navigation. Magnetic resonance in medicine: official journal of the Society of Magnetic Resonance in Medicine / Society of Magnetic Resonance in Medicine. 2013 Apr 8.
18. Lustig M, Pauly JM. SPIRiT: Iterative self-consistent parallel imaging reconstruction from arbitrary k-space. Magnetic resonance in medicine. 2010; 64(2):457–71. [PubMed: 20665790]
19. Uecker M, Lai P, Murphy MJ, Virtue P, Elad M, Pauly JM, Vasanawala SS, Lustig M. ESPIRiT-an eigenvalue approach to autocalibrating parallel MRI: Where SENSE meets GRAPPA. Magnetic resonance in medicine. 2013; 1001:990–1001.
20. Rapacchi S, Han F, Natsuaki Y, Kroeker R, Plotnik A, Lehrman E, Sayre J, Laub G, Finn JP, Hu P. High spatial and temporal resolution dynamic contrast-enhanced magnetic resonance angiography using compressed sensing with magnitude image subtraction. Magnetic resonance in medicine. 2014; 71(5):1771–83. [PubMed: 23801456]

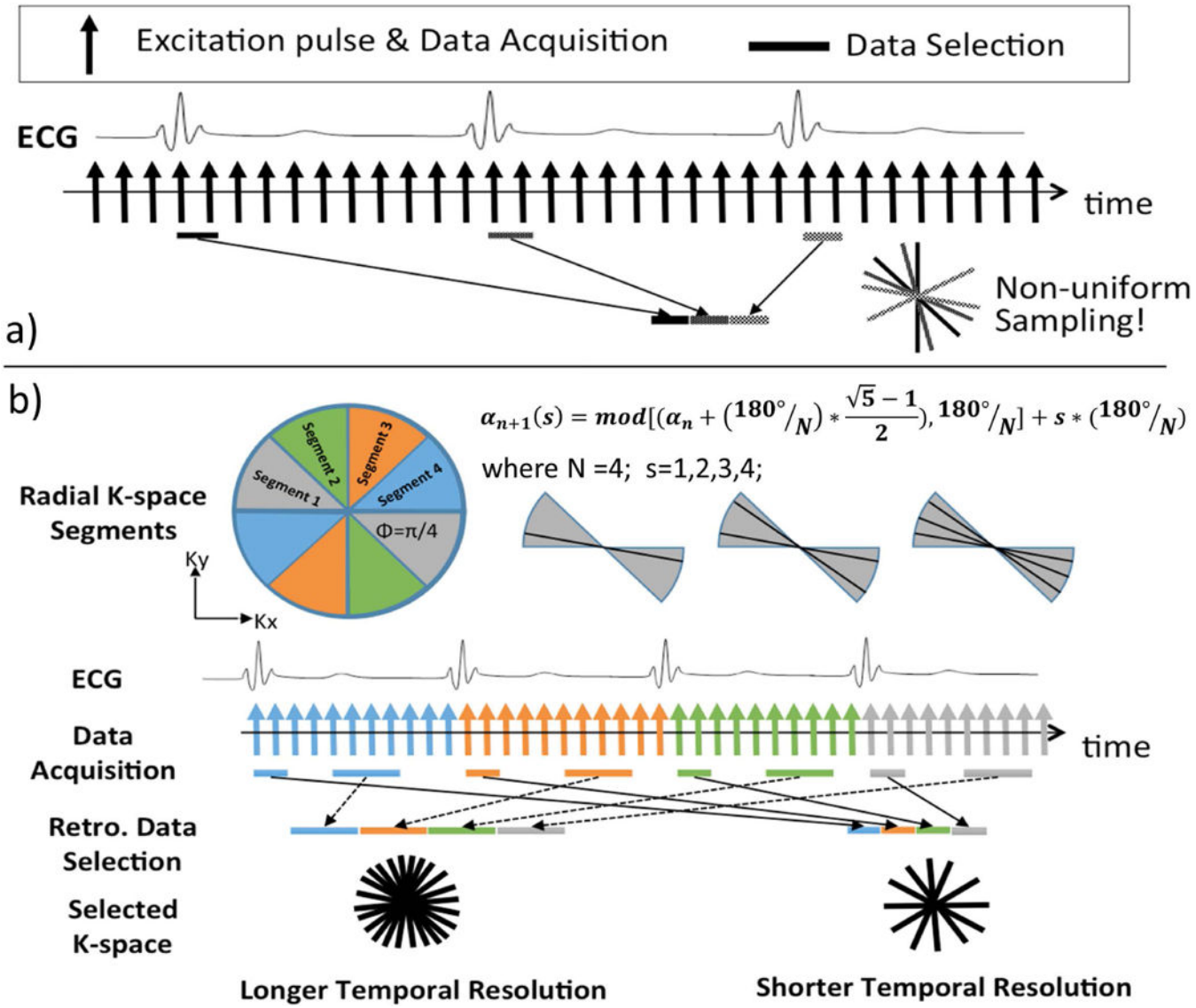

Figure 1.

Illustration of (a) the conventional golden ratio method when applied with ECG-gated segmented acquisition, which results in non-uniform sampling of k-space; and (b) the proposed segmented golden ratio method addresses non-uniform sampling by performing golden ratio acquisition inside each segment of a single heartbeat. The latter method (b) could provide near-uniform k-space sampling of arbitrary acquisition window length and position within a cardiac cycle.

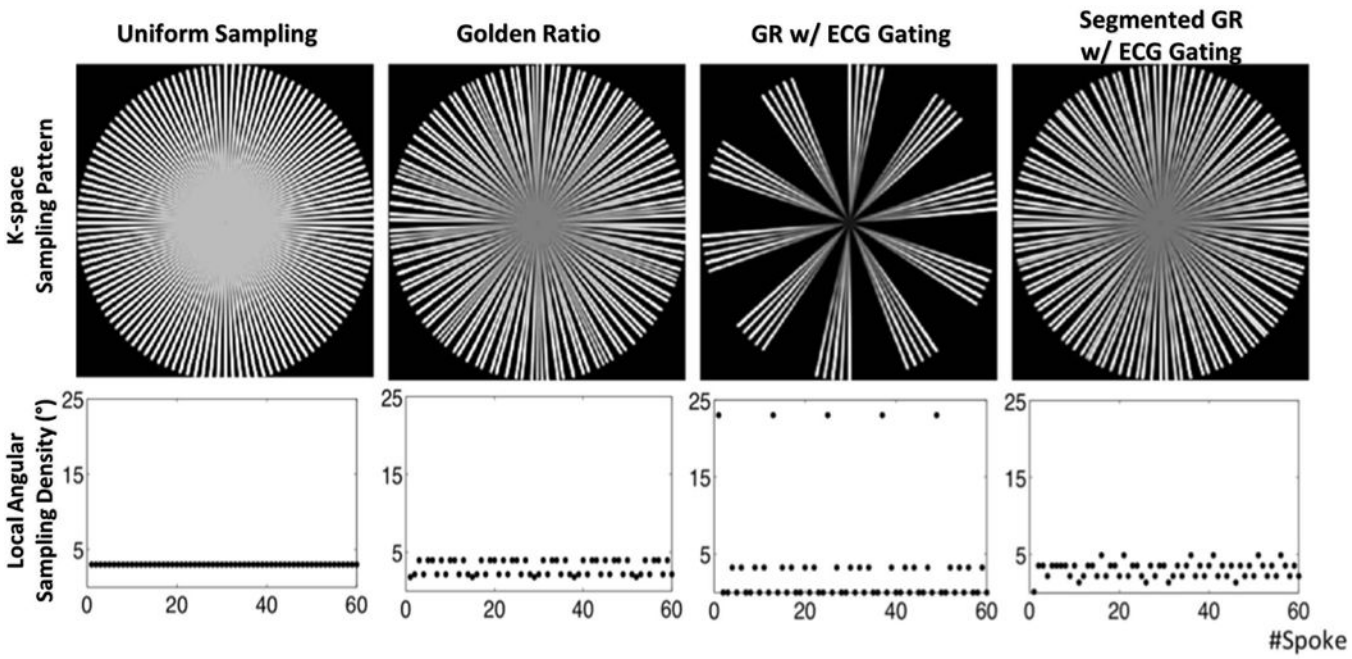

Figure 2.

The k-space sampling pattern and local angular sampling density of computer simulations on different reordering methods with N=60. In non-ECG-gated methods, both uniform sampling and conventional GR provides near-uniform sampling of the k-space. In cases with ECG gating, large gaps exist in the k-space sampling pattern of conventional GR while the proposed segmented GR method provides a near-uniform sampling pattern, similar to the one without ECG-gating.

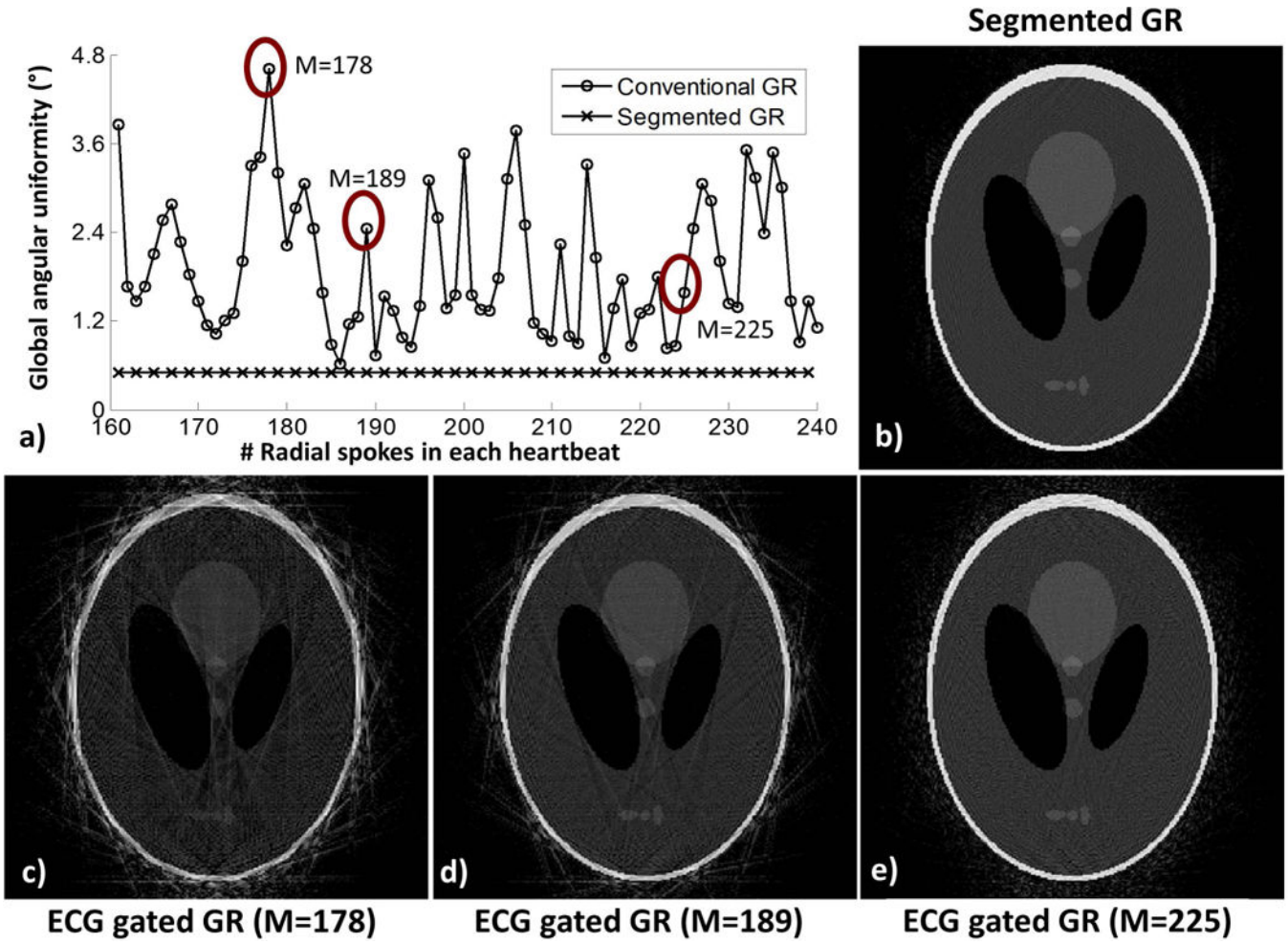

Figure 3.

(a) The k-space global angular sampling uniformity of ECG-gated GR (K=96, 12 simulated heartbeat) is dependent on the number of radial spokes within each heartbeat while the proposed segmented GR radial technique provides a much more uniform k-space sampling pattern. The reconstructed images (c–e) using the sampling pattern of conventional ECG-gated GR when M=178, M=189 and M=225 have variable degree of streaking artifacts due to non-uniform k-space sampling while the images obtained from segmented GR (b) have minimal streaking artifacts.

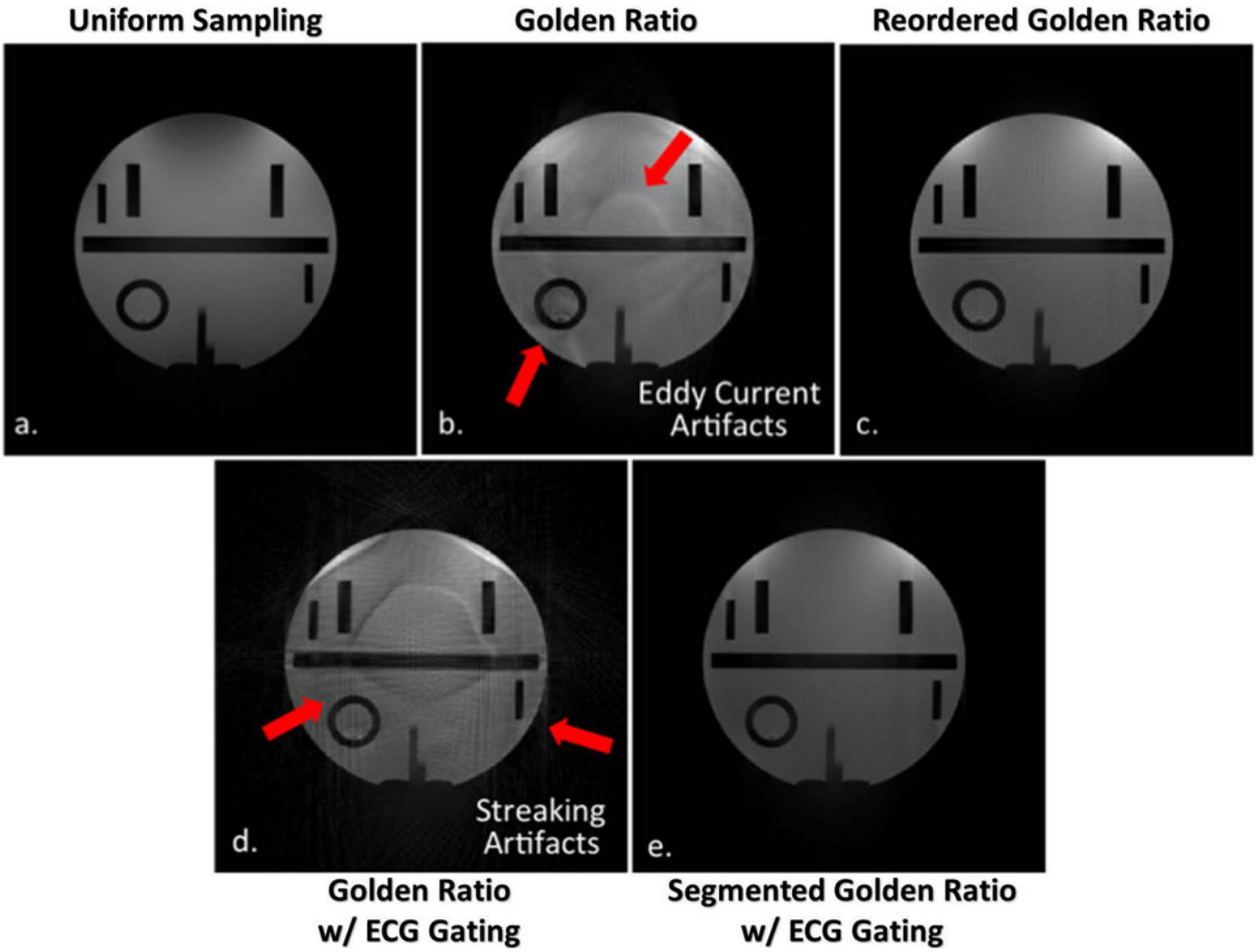

Figure 4.

Reconstructed images from phantom imaging experiments. The results correlate well with computer simulations where the streaking artifacts that are presented in the conventional ECG-gated GR method (d) are removed in the proposed segmented GR method (e). Moreover, the additional imaging artifacts in conventional GR methods (b, d) are completely removed in the proposed method (e) and non-ECG-gated reordered GR (c) where an identical sampling pattern, but a different reordering is used.

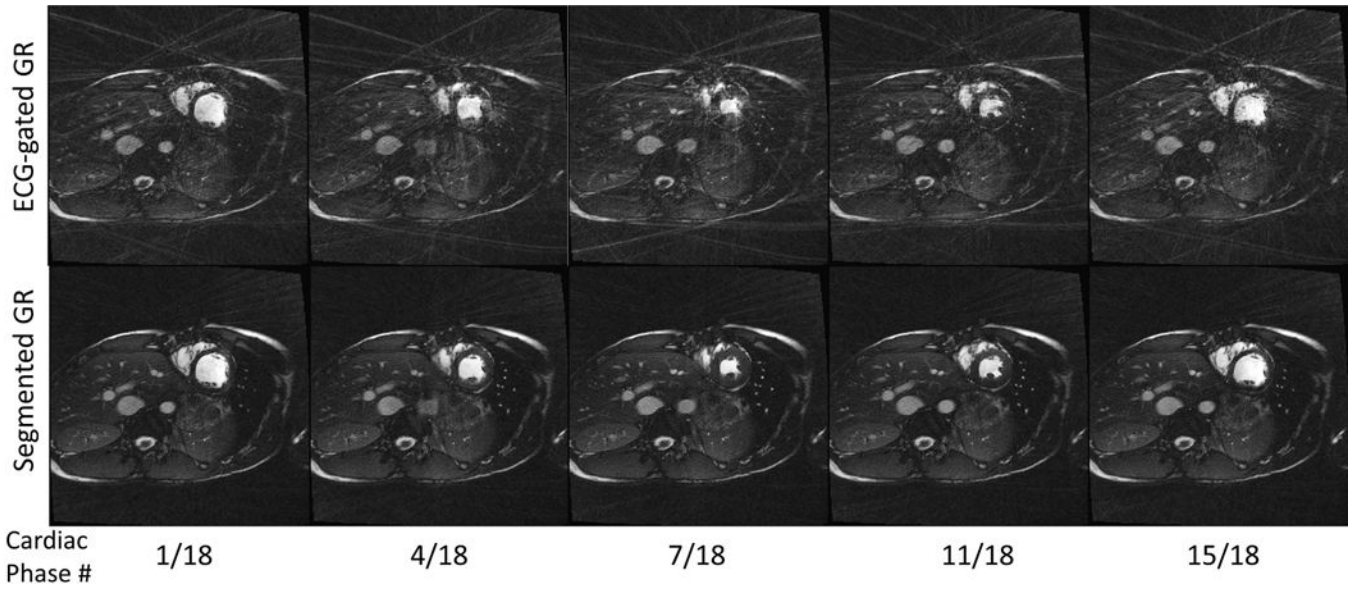

Figure 5.

Comparison between 2D radial ECG-gated cardiac cine images using the proposed segmented GR (bottom row) and conventional GR (top row). Five out of 18 cardiac phases are chosen for display. Severe streaking artifacts due to the non-uniform sampling of the k-space found in conventional GR are absent in the reconstructed images using the proposed segmented GR method.

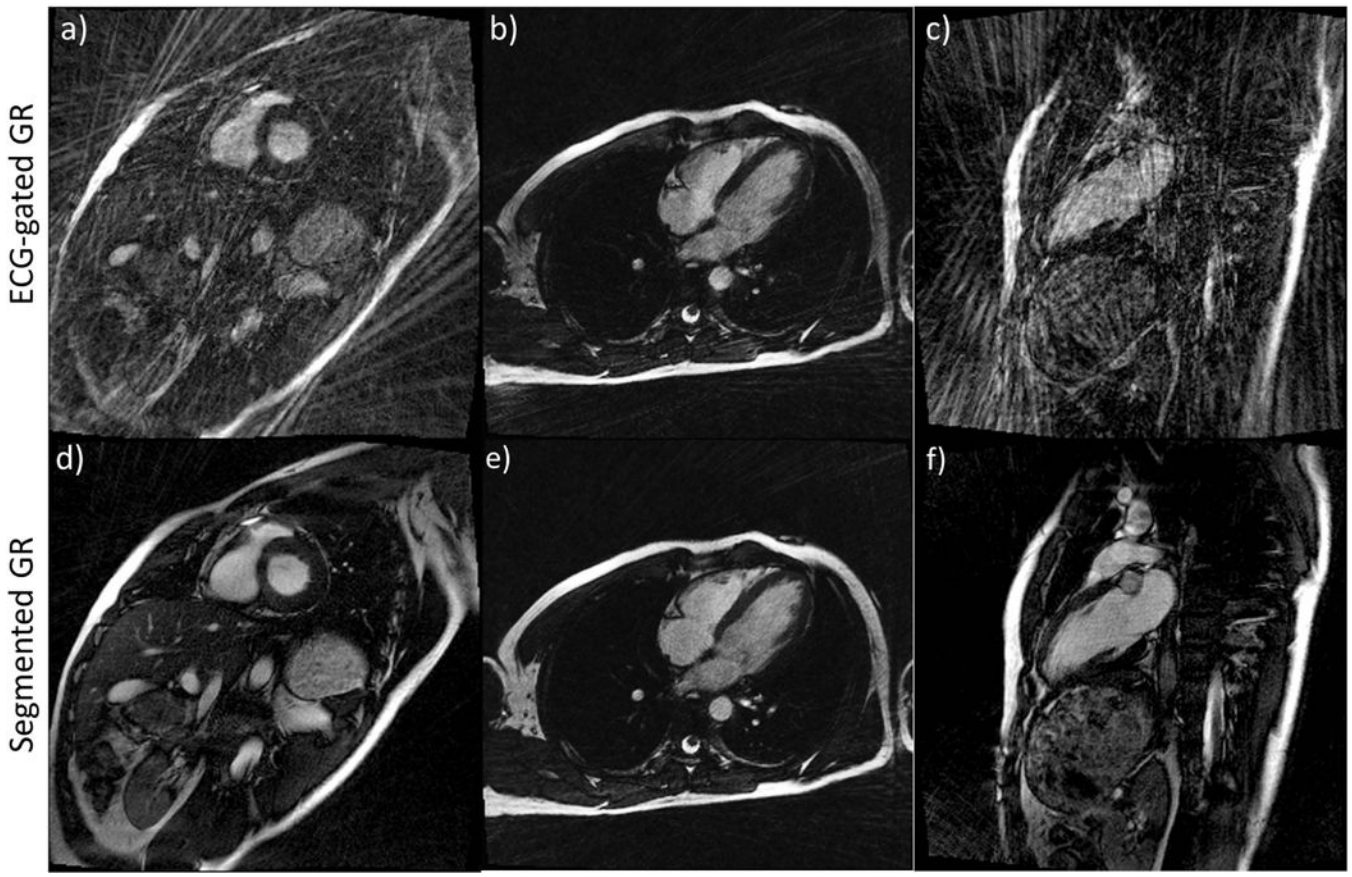

Figure 6.

2D Cardiac cine images in short axis (a, d), horizontal long axis (b, e) and vertical long axis (c, f) of the same subject using conventional GR (a, b, c) and the proposed segmented GR method (d, e, f). Due to small variations in the heart rate, the image quality of conventional GR is unreliable (a–c). Compared to conventional GR, the proposed segmented GR method generated images with uniformly good quality and minimal streaking artifacts. All images are reconstructed using same number of radial spokes. Corresponding CINE movie is available as Supporting Video S1.

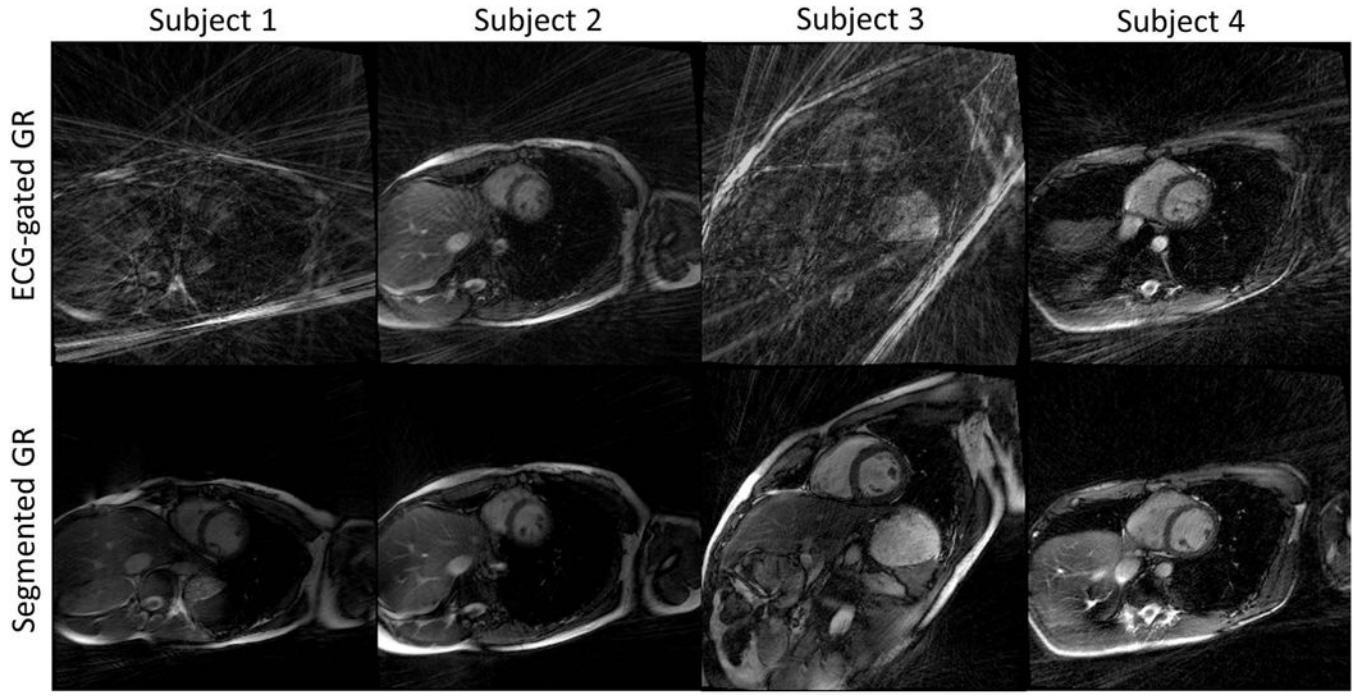

Figure 7.

3D cardiac CINE short axis images of four healthy volunteers. The images generated from conventional GR (subject 1 and 3) are non-diagnostic due to severe streaking artifacts. The images using segmented GR method provide uniformly good quality even though the same number of radial spokes were used.

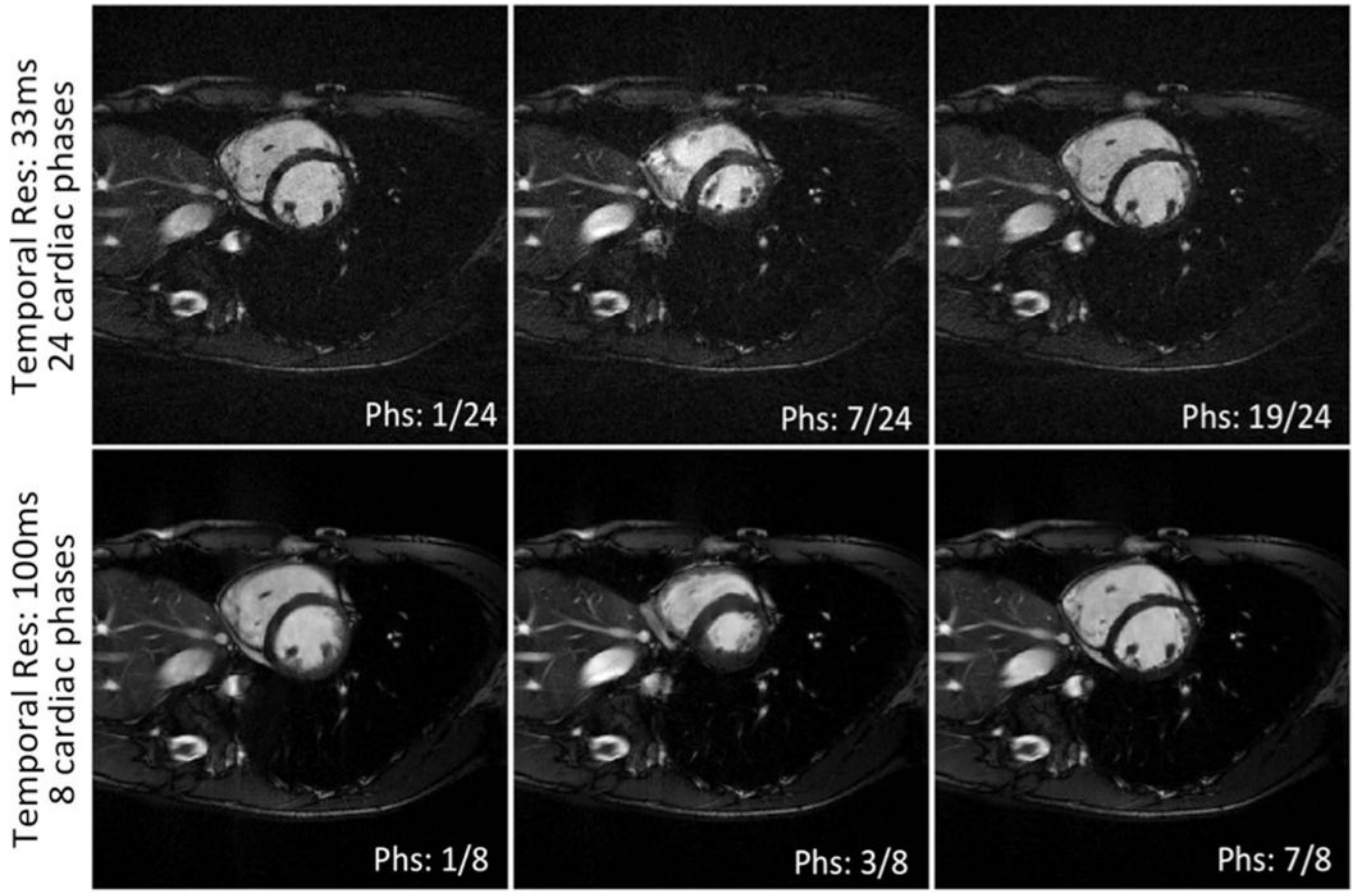

Figure 8.

Image quality with retrospective determination of temporal resolution using one 2D cardiac CINE dataset: a) 24 cardiac phases with temporal resolution of 33ms and b) 8 cardiac phases with temporal resolution of 100ms. Corresponding CINE movie is available as online Supplementary material. Corresponding CINE movie is available as Supporting Video S2.

Table 1

Global angular sampling uniformity (°) of radial spokes with number of spokes K=60, 96, 144, 192 (M=200).

	K=60	**K=96**	**K=144**	**K=192**
Uniform	0.00	0.00	0.00	0.00
Golden Ratio (GR)	0.95	0.46	0.70	0.64
ECG gated GR	**6.73**	**3.30**	**1.57**	**1.39**
ECG gatedSegmented GR	1.01	0.48	0.40	0.03

Table 2

Subjective image quality scores on 2D and 3D cardiac CINE using conventional GR and segmented GR radial scanning. SA: short axis. VLA: vertical long axis. HLA: horizontal long axis.

Conv. GR / Seg. GR	SA apex	SA mid	SA base	VLA	HLA	3D SA
Subject 1	2 / 4	1 / 5	1 / 4	2 / 4	1 / 5	1 / 4
Subject 2	1 / 4	1 / 5	1 / 5	1 / 3	2 / 4	1 / 5
Subject 3	2 / 4	2 / 4	1 / 4	1 / 5	1 / 4	2 / 4
Subject 4	1 / 4	1 / 4	2 / 4	1 / 4	1 / 4	1 / 4
Subject 5	2 / 4	3 / 4	3 / 5	1 / 3	3 / 4	1 / 4
Subject 6	3 / 5	2 / 5	4 / 4	3 / 4	2 / 4	2 / 3
Subject 7	2 / 4	2 / 4	2 / 4	1 / 4	2 / 4	3 / 5